

Applying interferometry to converted wave statics

David C. Henley and Pat F. Daley

ABSTRACT

In recent years, a wide variety of seismic processing techniques has appeared in the geophysical literature under the general heading of ‘seismic interferometry’. Most of the algorithms are for producing images from sets of seismic traces recorded using either well defined sources or random background microseisms, and all are characterized by the procedure of cross-correlating raw traces and, usually, summing the correlations over spatial apertures. In fact, it’s the cross-correlation that most specifically distinguishes interferometry from other seismic imaging techniques; and its purpose is to zero some common part of the phase difference between the input traces. Our ‘statics deconvolution’ method embodies the interferometric principle to remove time/phase differences in seismic traces recorded with common sources, receivers, or near-surface raypaths. Here, we attempt to use interferometry to correct converted wave seismic data for near-surface effects along the shear wave portions of the seismic propagation paths. Preliminary results show that we can improve the coherency of stacked converted wave events, but that preserving geologic structure is an unsolved problem. Likewise, we find some encouragement for the use of methods not involving ‘pilot traces’ but these methods need to be further developed.

INTRODUCTION

Many of us are more familiar with optical interferometry than the currently evolving technology of seismic interferometry, though the principles upon which both are based are quite similar. In optical interferometry, monochromatic light from a single source is split into two raypaths of equal length and recombined at a target receiver, where the constructive and destructive interference of the light waves creates a set of interference ‘fringes’, with the central peak being the brightest. Any disturbance of either light path, by changing its length slightly, or interposing an object, causes the interference fringes to shift spatially at the receiver, hence giving a sensitive measure of the transit time/phase disturbance caused by the perturbation. The interference pattern, or ‘fringe’, of the undisturbed system is just the autocorrelation of the source light wave, while the fringe of the system with perturbation is a cross-correlation embodying the time shift/phase difference caused by the perturbation.

In the introduction to a special supplement to *Geophysics* on the topic of seismic interferometry, Wapenaar et al (2006) provide a useful summary of the more recent applications of interferometry to seismic processing. In this introduction, the authors classify the applications according to whether they use measurements of diffuse wavefields, as in earthquake and passive seismology, or deterministic wavefields with man-made sources, as in exploration seismology. They then further distinguish interferometric techniques by their goals: Green’s function reconstruction; redatuming; or imaging. All of these methods share in common the use of autocorrelations and cross-correlations of raw data traces, and most invoke the reciprocity principle for seismic traces to motivate the use of these correlation functions. The latter principle justifies the

use of ‘time-reversed’ traces as filter functions to convolve with themselves and other raw traces to remove the phase of transmission effects.

The method we describe here is most closely related to redatuming, particularly that described by Bakulin and Calvert (2006) in their ‘virtual source’ method. In 2007, Henley and Daley (2007) showed the mathematical similarity between a modified virtual source method and the ‘statics deconvolution’ method as practiced by Henley (2004). The method of Bakulin and Calvert uses recorded traces of transmitted energy from surface sources to a borehole receiver to create virtual source gathers in which the virtual source is located beneath the near-surface complexities. The process involves cross-correlating a selected trace (gated over the early part of the trace to capture near-surface transmission response) with a common receiver gather, then summing these functions over an aperture to form a single trace for a virtual source gather. Each new selected trace, correlated with the same receiver gather and summed, provides a new trace for the output source gather.

To extend the method of Bakulin and Calvert to reflection data, we assume that a window of reflections on a seismic trace would include convolved surface response functions from both the source and receiver ends of the transmission path. We then assume that a band of reflections is only slowly varying laterally (this obviously excludes data sets with significant short wavelength structure). We then use a selected trace (gated over the reflection band) to cross-correlate a receiver gather, then sum the correlations into a single output trace for a source gather. We repeat the process to create a full suite of virtual source gathers, except that these gathers will still have near-surface disturbances attributable to the receivers. If we then sort the data into source gathers, we can repeat the above procedure; gating a selected trace around the band of reflections, correlating it with a source gather and summing to form one trace of a receiver gather. Repeating this procedure to form a complete set of receiver gathers should result in a data set free of near-surface disturbances, including static delays and scattered energy of all sorts.

One problem with the approach is that a cross-correlation is a bandlimiting operation; so bandwidth is lost with each correlation, unless compensation of some sort is applied. We find that two different techniques can compensate for the bandlimiting effect. One method consists of deriving a broadband match filter for each cross-correlation function and using the match filters to de-phase the raw traces; while the other consists of deriving an inverse filter for each cross-correlation and using the inverse filters to de-phase the input traces.

As described in earlier work (Henley, 2004), the ‘statics deconvolution’ method uses correlations of raw traces, not with themselves, but with ‘pilot’ traces consisting of stacks of raw traces. These correlations are non-linearly whitened, then used either as match filters to remove the near-surface effects of their corresponding traces, or used to derive inverse filters to remove the effects.

In our comparison of the modified virtual source method to statics deconvolution (Henley and Daley, 2007), we used a single data set as an example, mainly because the data were unique in having virtually no receiver statics over the relatively short receiver

spread (750 m), but visible source statics over the 6 km of the source spread. This means that we needed to apply the virtual source technique only once, on the source side, since receiver statics were considered negligible. Likewise, the statics deconvolution method needed only application to the receiver gathers.

In the present study, since we're considering converted wave data, we are eventually faced with application of the statics deconvolution method to both source gathers and receiver gathers, since the near-surface effects are quite different for the downgoing P waves than for the returning S waves.

PROPOSED METHOD DETAILS

The input data for the interferometric statics techniques is raw shot gathers with elevation statics applied and any coherent noise attenuated. Since we're looking only for effects related to the near-surface, we remove normal moveout as accurately as possible, at least for the windowed event sequence chosen for analysis. Also our methods are focused primarily on improving the S/N and coherence of converted wave events, but we have made no effort to account for geological structure and to separate it out from near-surface effects.

In previous work (Henley 2007, 2008) we have applied interferometry methods without invoking surface-consistency; most notably in the 'raypath interferometry' method, where we transform input gathers into the radial trace domain, thus mapping data into the apparent velocity/injection angle domain. For our venture into converted wave statics, we allow the use of surface-consistency, if warranted, but do not insist on it. Hence, one of the data ensembles we consider for interferometric picking of 'statics' is either common shot stack or common receiver stack panels. If the receiver shear wave statics are at all large, however, we expect the common shot panel to be minimally useful, and we then attempt to pick individual gathers. A 'bootstrap' method which might help is to first form the common receiver stack panel, assuming shot statics are relatively small, then to pick the receiver stack panel and apply its correction functions to the individual receiver gathers. The common shot stack panel can then be formed and picked in turn, in order to apply its correction functions to the individual shot gathers.

If this method fails, we attempt to pick individual gathers in both shot and receiver domain. In either case, we face the issue of forming pilot trace panels against which to pick either the common shot/receiver stack panels, or the individual shot/receiver gathers. Our success in earlier work has depended largely upon our success in constructing appropriate pilot trace panels. What has worked best has been to hand-pick a horizon on the best available brute stack of the input data, to use the horizon file to flatten the individual panels to be picked, to mix the flattened panels over a wide aperture, to remove the flattening, and to use the resulting smoothed panels as the pilot traces for the raw panels from which they are derived.

The actual interferometric static correction works as follows: each trace of a raw input panel is cross-correlated against its corresponding pilot trace; the correlation function is non-linearly whitened (samples raised to an odd power), and the function is then either convolved directly with its corresponding raw trace; or an inverse filter is derived for the

correlation and the inverse filter applied to the raw trace to reverse the phase of the correlation. This technique has several advantages: if the correlation window is large enough, the function will capture quite large statics; multi-path events and short-period multiples are automatically included; there is no need to ‘pick’ a single correlation peak in order to isolate a single time shift to apply to the trace. The main disadvantage is that if the traces are noisy, the bandwidth of the resulting correlations and inverse filters may limit the band of the data to which they are applied.

To use surface-consistency with interferometry, we can form common shot and common receiver stacks as described above; but if the statics are large, that method may fail. Another approach is to pick individual shot and receiver panels against their corresponding pilot trace panels, then to sum the correlation functions over common shot and common receiver before whitening them or deriving inverse filters.

Ultimately, since pilot trace methods can lead to false events in noisy zones of stacked sections (Ursenbach and Bancroft, 2000) unless due care is exercised, we would like to be able to use only cross-correlations of raw traces for input to interferometric correction methods. While many methods involving correlations of raw traces are possible, we examine only one in this work; the so-called ‘differential’ method, wherein we use adjacent trace correlations to derive corrections between traces. Our interferometric approach introduces one complication into the differential approach, however. When we use adjacent trace correlation peaks to find the time shifts between adjacent traces, the total trace statics are obtained by summing the individual shifts from the beginning of a picked trace ensemble. Thus the second trace in an ensemble would have a single correlation shift applied; the third trace would have the sum of the first two correlation shifts applied; the fourth trace is shifted by the sum of the first three correlation shifts; and so forth. When we use the correlation functions to derive inverse filters for correcting traces by deconvolution, however, we can’t simply sum them to derive the total statics functions for successive traces in an ensemble. Instead, we should convolve the second trace by the inverse filter for the first trace pair correlation, then convolve the third trace by the inverse filters for both the first and second trace pairs, and so forth. This would quickly lead to severe bandlimiting due to the number of successively convolved inverse filters; so we attempt only to address the shortest wavelength corrections by applying the single inverse filters for adjacent trace correlations.

TEST RESULTS

The Spring Coulee data have been processed conventionally by Han-xing Lu (2008) of the CREWES staff, including laborious hand-derivation of converted wave statics. Figure 1 shows the excellent CCP stack of the inline horizontal component of these data, as obtained by Han-xing. This will provide a standard for comparison as we test what we hope will be more hands-off approaches to converted wave statics. In all our tests, we apply the elevation and P-wave (source) statics derived by Han-xing to the raw trace gathers that we use as input for our tests. In this way, we will only be searching for the large and difficult S-wave (receiver) statics still residing in the gathers. One thing to note in Figure 1 is that fact that the S-wave statics appear to have corrected the shallower band of events at around 800 ms reasonably well; but there appear to be unresolved statics issues for deeper events, evidence that statics are probably not stationary.

A difficulty that we encountered early in the data analysis was that of re-binning the gathers to CCP gathers. We found the ProMAX module used by Han-xing for that purpose was unable to handle our input gathers after being modified by our test processing. Therefore, we approximated CCP gathers by computing a nominal conversion point for each trace for the prominent event at 800 ms, eventually locating the CCP for each trace as $2/3$ the distance from source to receiver. We then stacked our processed gathers both by CDP and then by approximate CCP. Because of this approximation, we can't compare our stacks point by point with Figure 1, but we can get an idea of event coherence and smoothness for the various events on the record, which is some measure of the success of our methods.

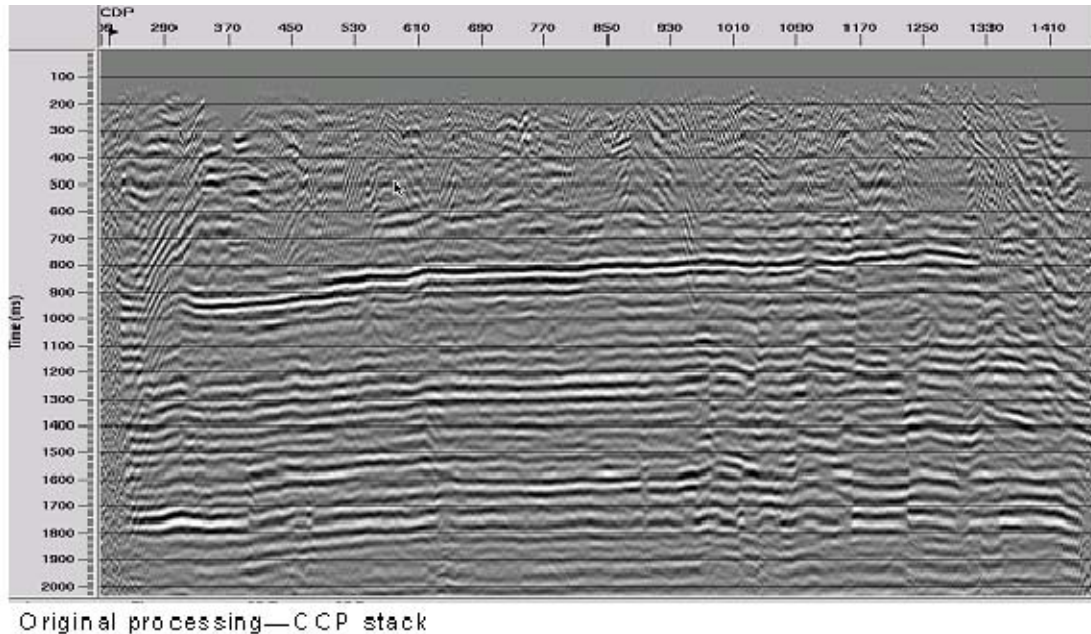
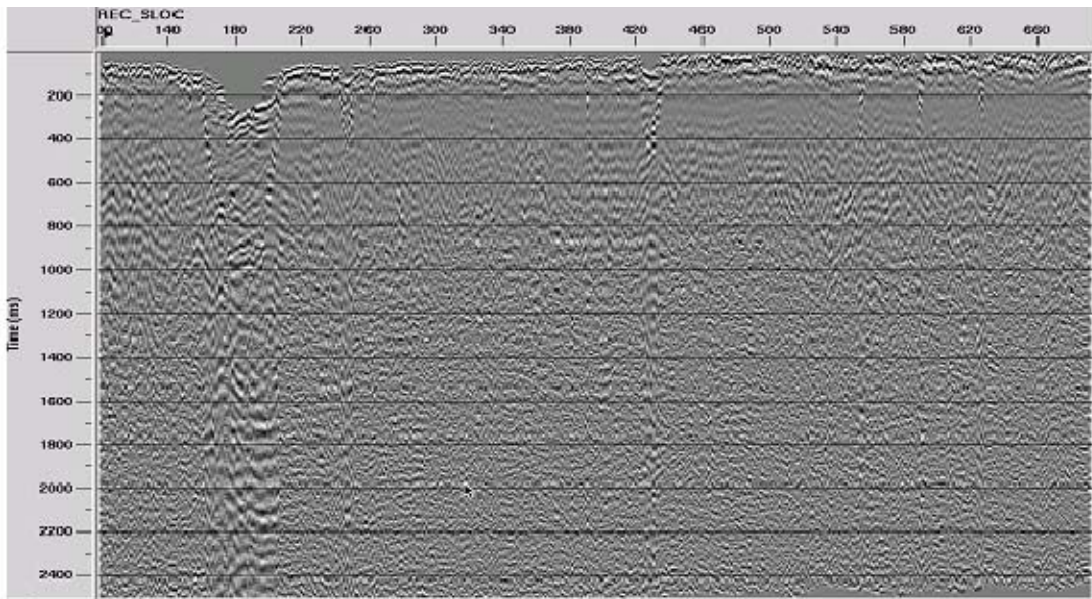


FIG. 1. CCP stack of inline horizontal component at Spring Coulee as produced by conventional techniques. The events near 800 ms are reasonably well corrected for S-wave statics, but deeper events appear less well corrected.

Since Figure 1 can only provide a partial test of the success of our techniques, we chose a second diagnostic to examine, as well. An obvious display for showing improvements in event coherence related to receiver statics or statics functions is the 'receiver stack', which is created by summing all the NMO-corrected traces in each receiver gather and plotting them as a function of surface location. Figure 2 shows the receiver stack for the raw traces with elevation statics and P-wave statics applied. Considering how little coherent signal we see in this figure, it should be easy to detect any improvements to the receiver stack produced by our methods. We show in Figure 3 a receiver stack where we have limited included traces to only those whose source-receiver offsets lie in the range of 100 to 1000 m. On this display, we can get some sense of the size and wavelength of the required corrections for both shallow and deep events.

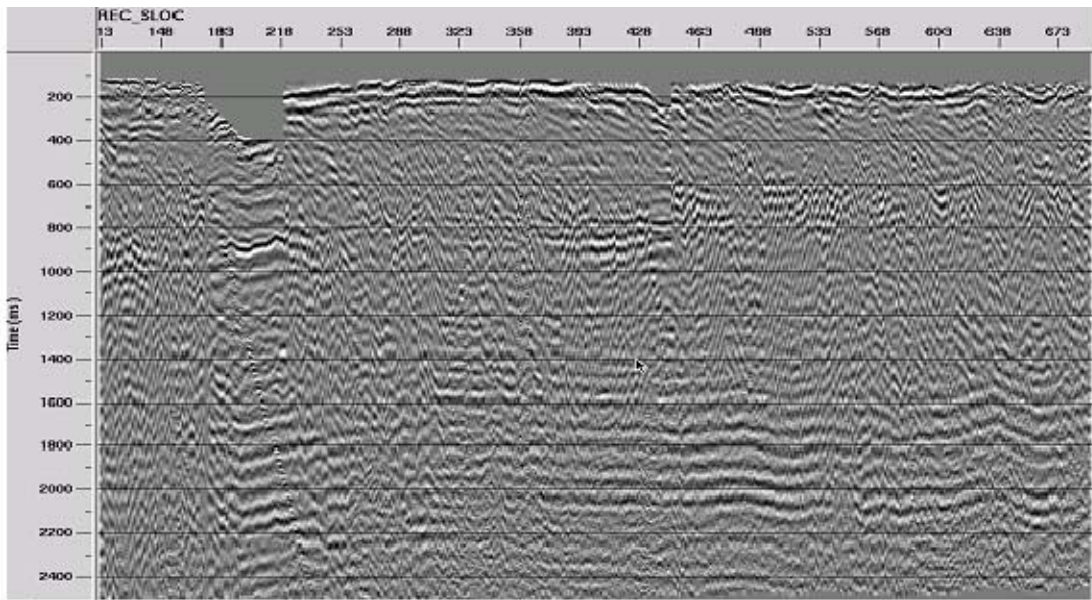
As suggested in our proposed methods section, we tried correlating traces on the common receiver stack with pilot traces created using a 'trim statics' approach to align

the receiver stack traces, then trace mixing to improve S/N. This approach failed badly, probably because we were unable to produce acceptable pilot traces from the receiver stack panel due to the short wavelength and magnitude of the apparent statics.



Receiver stack from decon shot gathers—all offsets

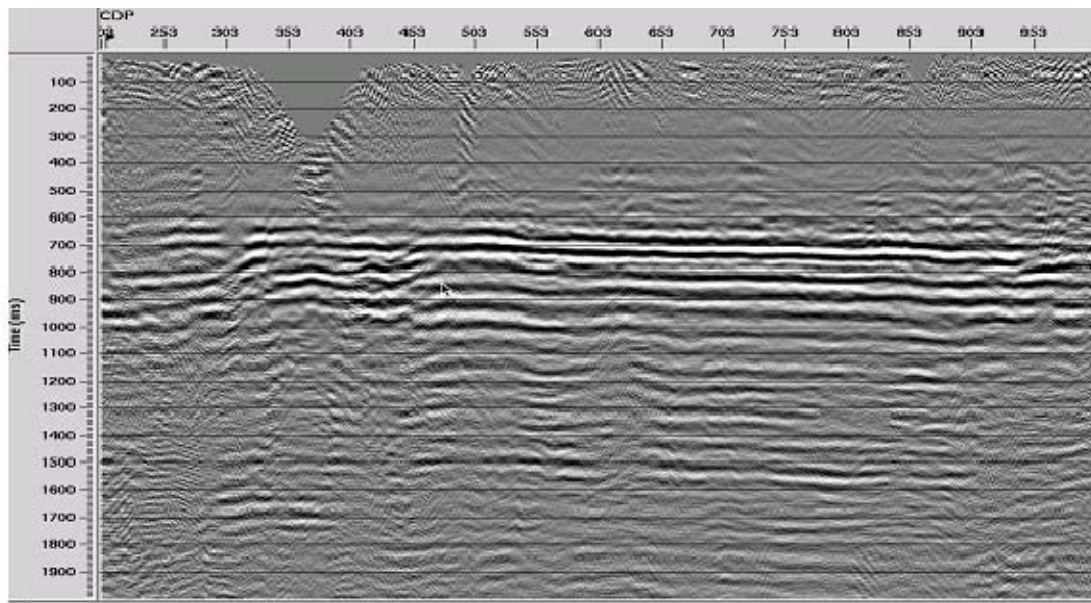
FIG. 2. Common receiver stack panel with all traces included—hardly any event coherence can be seen.



Receiver stack from decon shot gathers, offsets 100-1000 m

FIG. 3. Common receiver stack including only traces with offsets between 100 and 1000 m. Enough event coherence can now be seen to discern the statics problems at all event levels. The events on this display show less dip than those in Figure 1, due to differences in statics.

Since we could actually see converted wave events on raw shot gathers, we attempted next to find receiver statics functions for each individual shot gather by creating pilot traces for each gather and correlating the raw traces with their corresponding pilot traces. To create the pilot traces, we used the ProMAX operation ‘Align events in window’ followed by a short wavelength trace mix operation to improve S/N of the pilot traces. A major drawback of this procedure is that it forcibly removes all relative shifts between traces in the input ensemble, including those due to geological structure. Also, we could not achieve acceptable event coherence unless we used a window which included only a narrow band of events, in this case those at 800 ms. This means that any statics functions derived would represent only the windowed events. Using this approach of correlating raw traces with their shot gather-derived pilot traces, we were able to create the CDP stack shown in Figure 4.



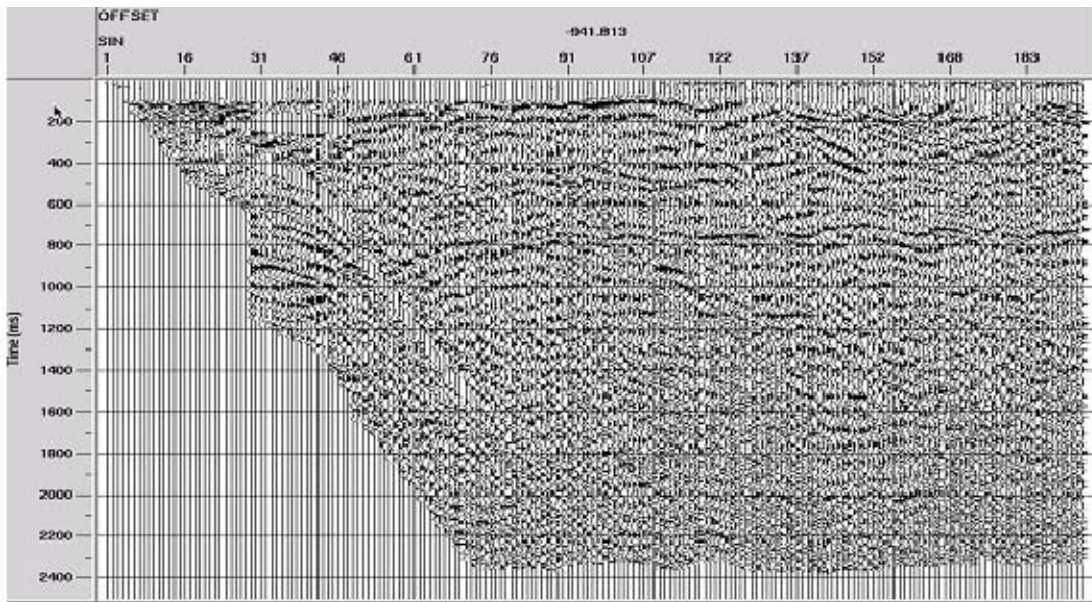
Interferometry on shot gathers—CDP stack

FIG. 4. CDP stack of shots corrected from correlations with shot-derived pilot traces. The events in this display do not reflect the same structural dip as those in Figure 1, possibly due to the difference in statics. While the interferometric ‘statics deconvolution’ approach appears to have greatly improved the event coherence and S/N for events around 800 ms, deeper events are less well enhanced.

Figure 4 shows that we can, indeed, improve the coherence and S/N of converted wave events using the ‘statics deconvolution’ approach. The relative confusion toward the left end of the line reflects the fact that the pilot trace method we have used does not honor geological structure; and the breaks in coherence of deeper events indicate that the required statics functions may not be surface consistent for at least some parts of this line. In order to accommodate non-surface consistency, we decided to use the raypath statics approach (Henley 2008), wherein surface corrections are derived from common-angle panels.

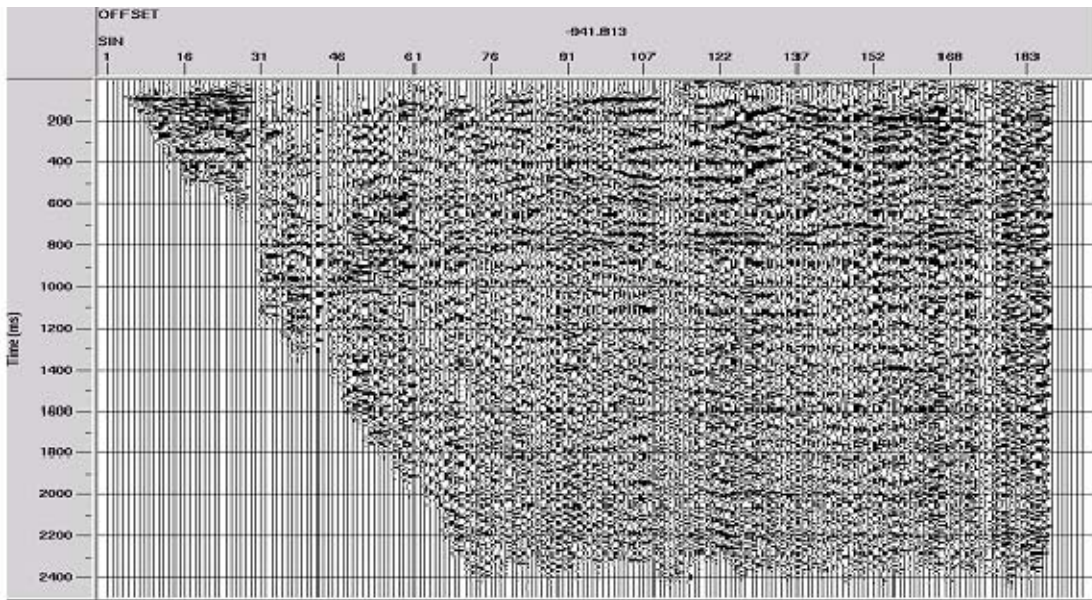
To create common-angle panels, we transform all the raw shot gathers to the radial trace domain, and sort the traces by apparent velocity (angle) and surface location. Each

panel is somewhat analogous to a common-offset panel in the XT domain, but tends to isolate coherent events by the angle at which their energy is transmitted or received at the surface. Our technique here is just to create pilot traces from the common-angle gathers in the same fashion that we did for shot gathers—by forcing event alignment in a window, applying a short trace mix to enhance S/N, then correlating raw common-angle traces with their corresponding pilot traces to derive the statics functions. The inverse filters derived from the statics functions are applied to the common-angle traces in each gather; then the common-angle gathers are re-sorted to radial trace gathers, and the radial trace gathers inverted to shot gathers. Figures 5 and 6 show a typical common-angle gather before and after the application of the inverse filters derived from the raw/pilot trace correlations. Interestingly, the S/N is higher on many common-angle panels than it is on the individual XT domain shot gathers from which they are derived. Figures 7 and 8 show a common-angle gather for a different apparent velocity before and after the interferometric procedure, and Figures 9 and 10 show yet another common-angle gather before and after correction. On all of these gathers, it can be seen that the overall alignment of the converted wave events improves after application of the inverse filters, although the panels are somewhat noisier after correction than before.



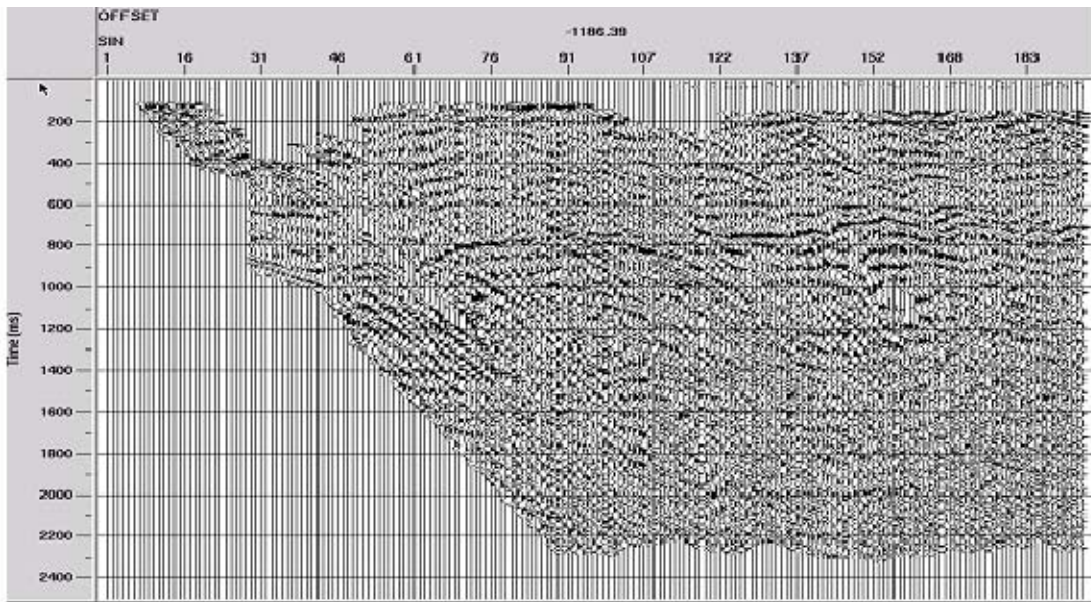
Typical common-angle gather before interferometric correction

FIG. 5. Typical common-angle gather for Spring Coulee inline horizontal component. Note the evident event variations due to surface effects, particularly on the event at 800 ms.



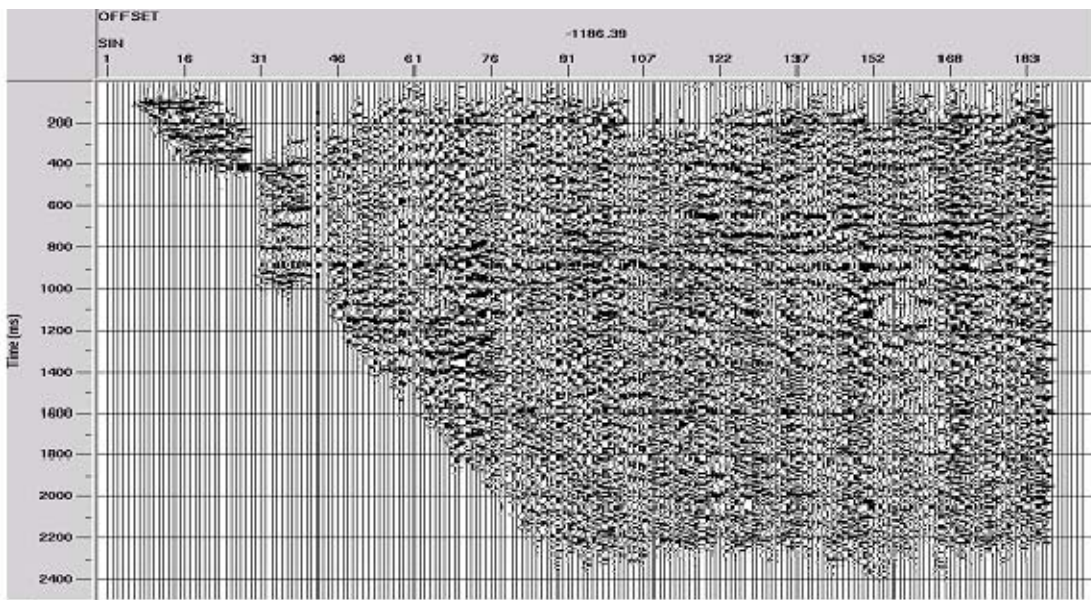
Common-angle gather after interferometric corrections

FIG. 6. Common-angle gather from Figure 5 after application of inverse filters derived from correlation statics functions. Both shallow and deep events are better aligned.



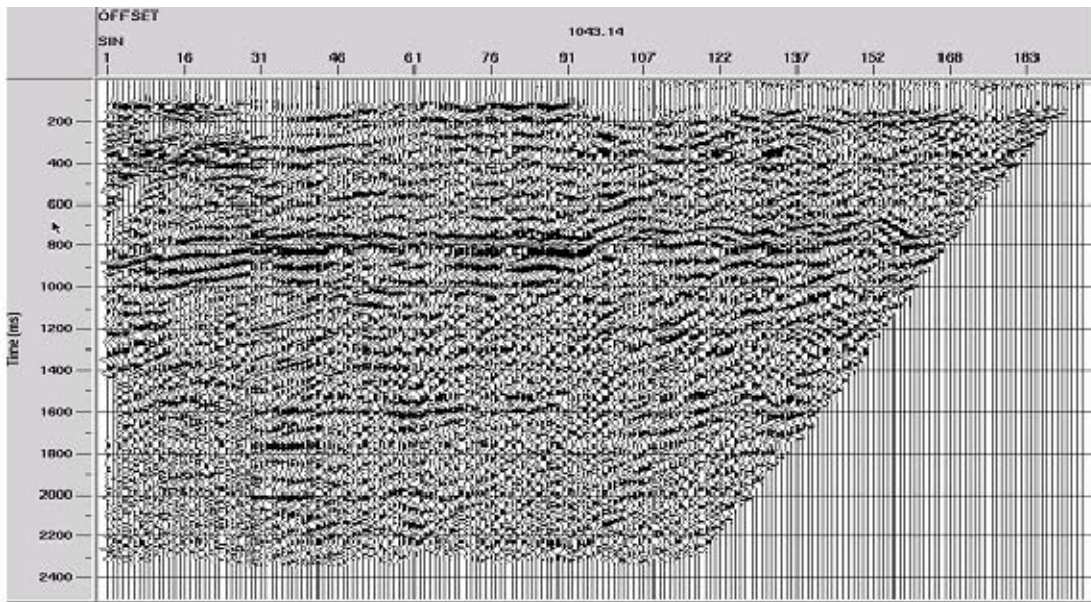
Typical common angle gather before interferometric correction

FIG. 7. Common-angle gather for a different apparent velocity (angle) before application of static deconvolution.



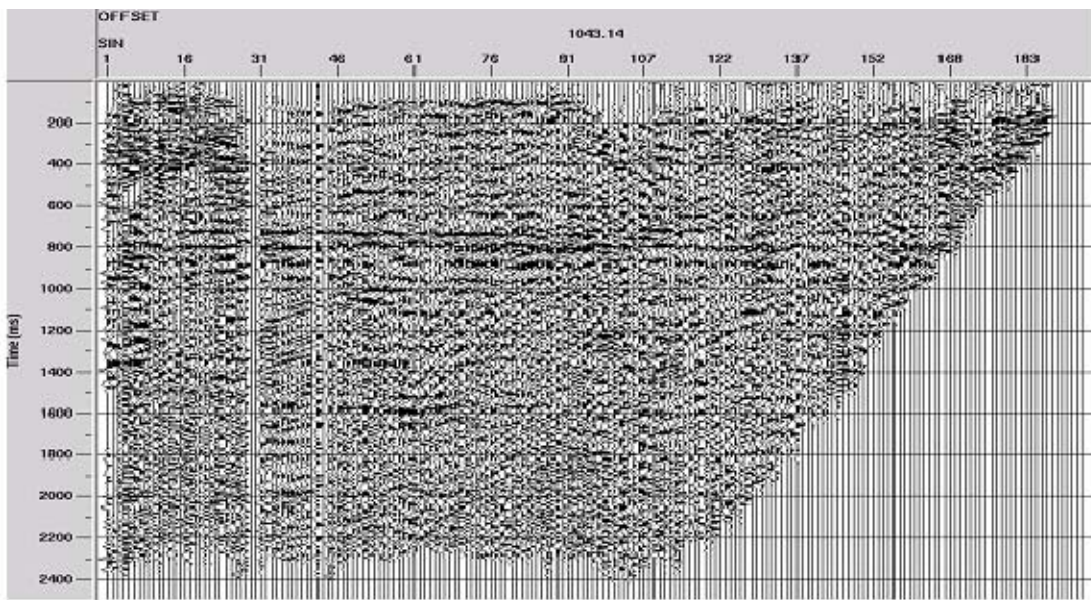
Common angle gather after interferometric correction

FIG. 8. Common-angle gather from Figure 7 after interferometric correction. Both shallow and deep events are better aligned.



Typical common angle gather before interferometric correction

FIG. 9. Common-angle gather with a different apparent velocity. Event S/N is better when viewed from this angle.



Angle gather after Interferometric correction

FIG. 10. Common-angle gather from Figure 9 after interferometric correction. The improved event alignment is more apparent on this gather due to the higher S/N.

The number of common-angle panels created for any seismic line depends strictly upon the choice of velocity increment in the radial trace transform; the finer the increment, the more panels, and the greater the redundancy of the wavefield represented in each individual common-angle panel.

After all the common-angle panels are corrected using the inverse filters derived from their corresponding statics functions, the panels are re-sorted to radial trace gathers and inverted to shot gathers. When we stack the corrected shot gathers by CDP, we get the image in Figure 11; and when we create approximate CCPs and stack the gathers by CCP, the image in Figure 12 results. Interestingly, the deeper events image better on the CCP stack, indicating that our raypath domain corrections seem appropriate for converted wave events.

Figure 13 offers another diagnostic on the interferometric approach applied in the raypath domain. The receiver stack displayed here shows that this approach has reduced the statics which are so apparent in Figure 3. Like the events in Figure 11, the alignment and coherence has improved the most for the shallower events. These are evidently the events which most nearly approximate surface consistency on the receiver end of the raypath.

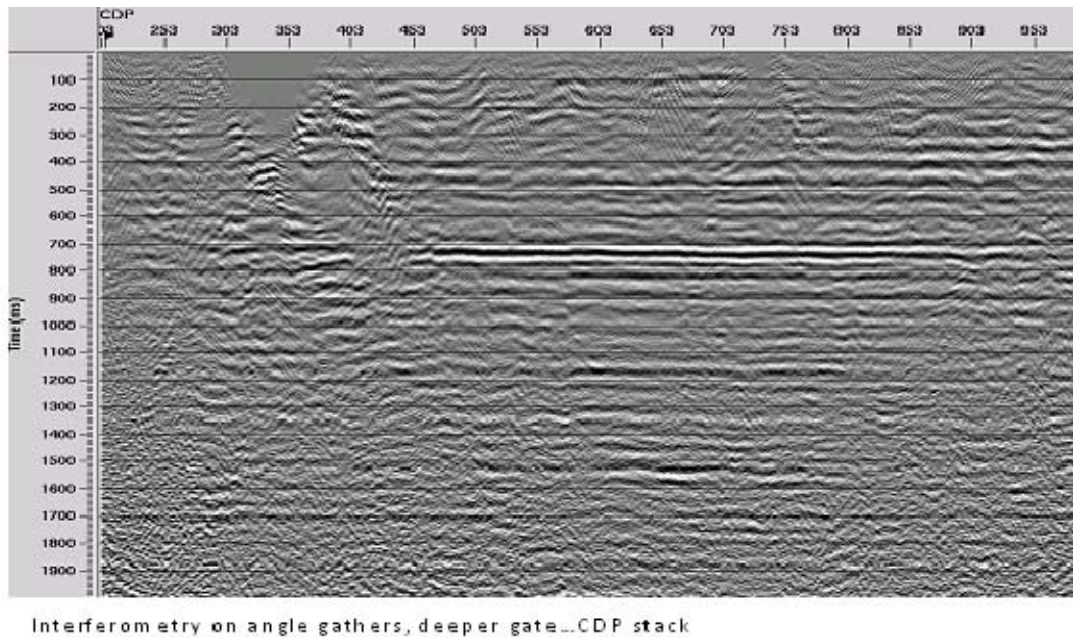
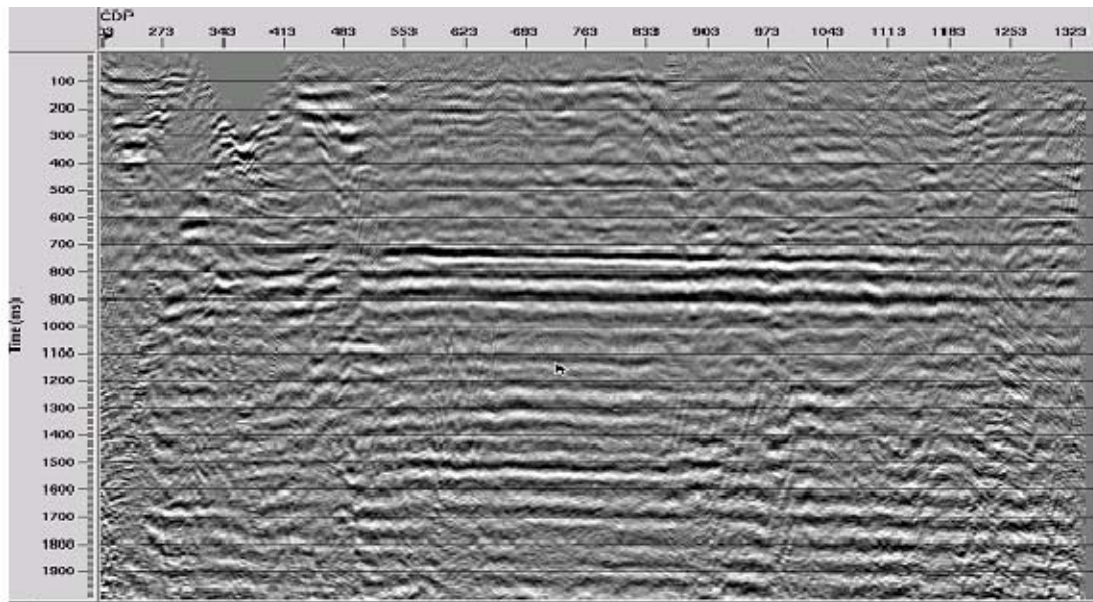
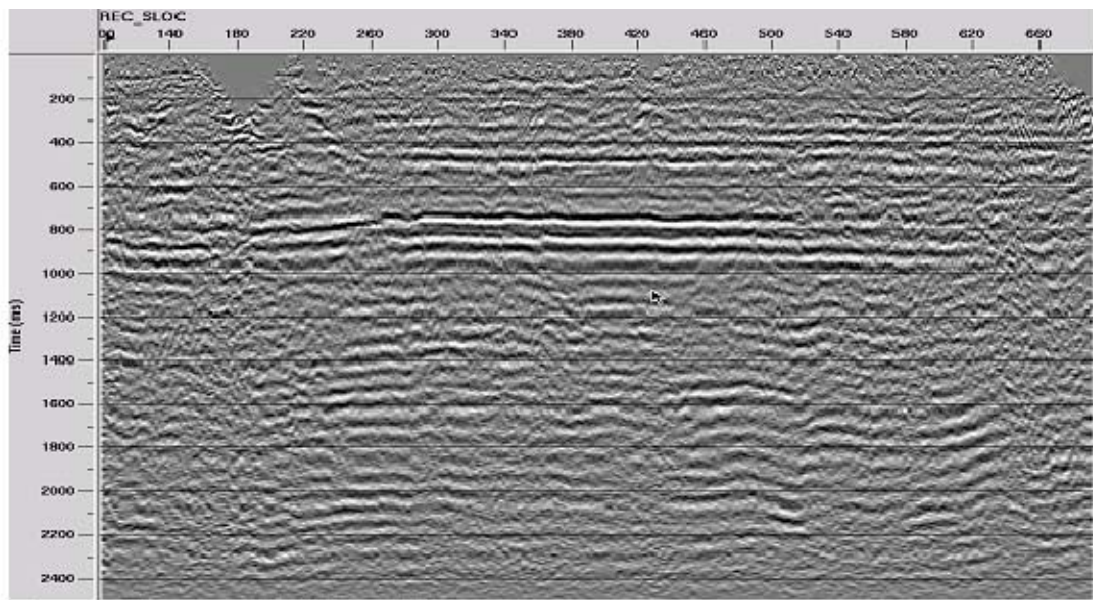


FIG. 11. CDP stack of shots corrected in the raypath domain by statics deconvolution. Geological structure is destroyed by this procedure, since the common-angle pilot trace creation process removes all structure. Event alignment and coherence is good for events at 800 ms and shallower, but decreases with depth. Event bandwidth is also preserved.



Interferometry on angle gathers—approximate CCP stack—event focused

FIG. 12. Approximate CCP stack of shots corrected in the raypath domain (Figure 11). Strength, alignment, and coherence of deeper events appears better in this image.



Receiver stack after interferometry on angle gathers—100-1000m offsets

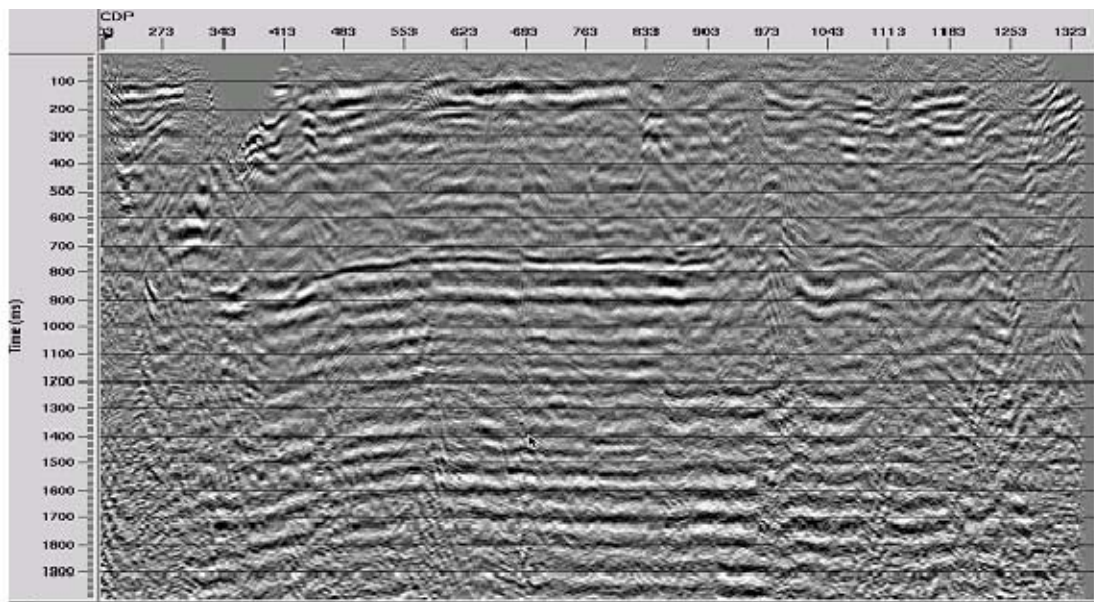
FIG. 13. Receiver stack after interferometric correction of common-angle gathers. Event alignment and coherence is improved over that in Figure 3.

PILOT-FREE METHODS

As we mentioned earlier, ultimately, we would prefer using a method which does not rely on the somewhat artificial device of pilot trace creation for its success. Our first attempt at such a method was applied in the raypath domain, just as the method described

above. Instead of artificially aligning all the traces in each common-angle gather and mixing them to provide pilot traces, we instead cross-correlate raw traces in consecutive pairs and derived inverse filters for these ‘differential statics functions’. Our first attempt at this differential approach resulted in the approximate CCP stack image in Figure 14. The receiver stack of these results is shown in Figure 15, which confirms that the method breaks down on the most difficult part of the line, where statics are large and S/N is reduced.

This result is only the first attempt at pilot-free results, and we hope to attempt other methods in the future; such as an iterative approach, or one starting with pilot trace guided corrections and refining these with a differential approach. Other techniques could be devised which use all possible trace pair correlations within a gather, rather than just nearest neighbor correlations.



Differential interferometry applied to angle gathers—no pilot—approximate CCP stack

FIG. 14. Differential interferometry applied to common-angle gathers before forming approximate CCP stack. The approach obviously breaks down on the portion of the line where statics are large. The geological structure of the line seems to be preserved, however.

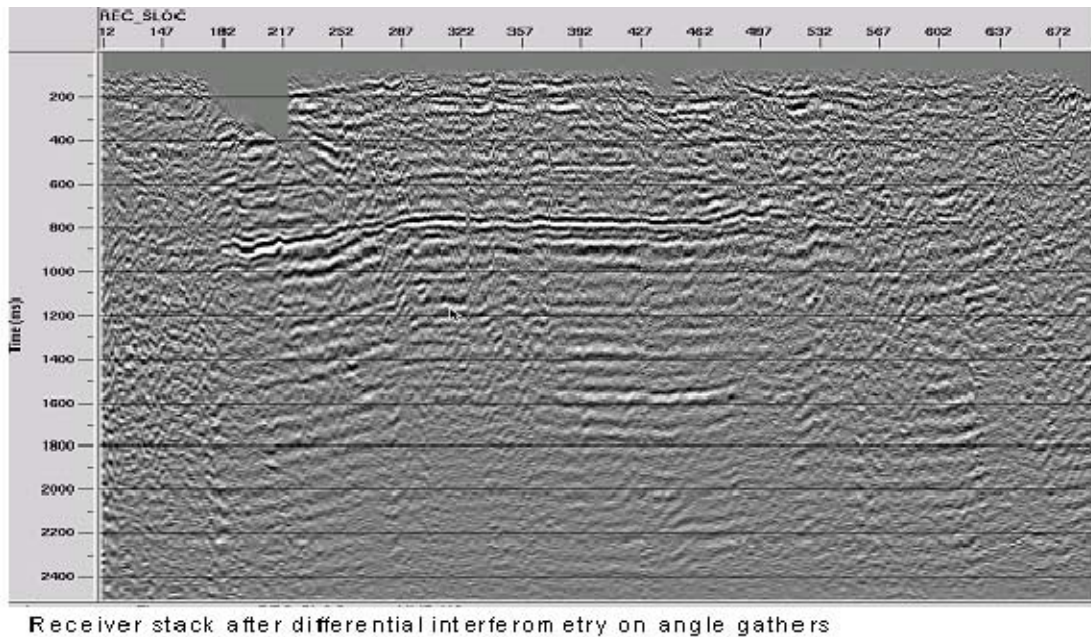


FIG. 15. Receiver stack of shots after differential interferometry applied to common-angle gathers.

CONCLUSIONS

Based on encouraging imaging results with an arctic data set having notoriously difficult statics problems, we attempted to adapt the interferometry or ‘statics deconvolution’ method to the problem of determining S-wave statics for converted wave events. We are in the early stages of testing various approaches to this difficult problem, but we have demonstrated that we can improve converted wave event coherence and continuity using statics deconvolution methods. Our experience has been that transforming the input data to the raypath domain (constant-angle panels created from radial trace transforms) provides corrections which improve the CCP imaging at all depths in the data. The same corrections applied before CDP stack were less effective on deeper events. Applying the corrections before receiver stacking was even less effective on the deeper events, but good for the shallow ones. This is indirect confirmation that the raypath approach is the appropriate one for converted wave data. Preserving geological structure properly remains a problem for our methods, but may be partially solved by developing techniques which don’t rely on pilot traces.

We also observed on these data that event coherence and S/N was much better on common angle gathers, particularly at certain angles, than it is on shot or receiver gathers, making them much easier to use as input for various picking or correlation methods. This phenomenon seems to occur on other data, as well.

ACKNOWLEDGEMENTS

The authors thank Han-xing Lu for the excellent processing on the Spring Coulee data which allowed us to perform our tests and analysis. We also acknowledge the continuing support of CREWES sponsors.

REFERENCES

- Bakulin, A. and Calvert, R., 2006, The virtual source method: theory and case study, *Geophysics*, **71**, S1139-S1150.
- Henley, D.C., 2004, A statistical approach to residual statics removal: CREWES Research Report, **16**.
- Henley, D.C., Bertram, Malcolm, Hall, Kevin, Bland, Henry, Gallant, Eric, and Margrave, G.F., 2006, The power of high effort seismic acquisition: the Longview experiment: CREWES Research Report, **18**.
- Henley, D.C., 2007, Raypath statics revisited: new images: CREWES Research Report, **19**.
- Henley, D.C., 2008, Raypath interferometry: statics in difficult places: 2008 CSPG CSEG CWLS Convention, expanded abstracts.
- Lu, Han-Xing and Hall, K.W., 2008, Preliminary processing results, Spring Coulee Alberta: CREWES Research Report, **20**.
- Ursenbach, C.P., and Bancroft, J.C., 2000, Noise alignment in trim statics: CREWES Research Report, **12**.
- Wapenaar, K., Draganov, D., and Robertsson, J., 2006, Introduction to the supplement on seismic interferometry: *Geophysics* **71**, S11-S14.